

Conformational Changes That Occur during an RNA-editing Adenosine Deamination Reaction*

Received for publication, July 5, 2001, and in revised form, July 27, 2001
Published, JBC Papers in Press, July 30, 2001, DOI 10.1074/jbc.M106299200

Hye Young Yi-Brunozzi, Olen M. Stephens, and Peter A. Beal‡

From the Department of Chemistry, University of Utah, Salt Lake City, Utah 84112

ADARs are adenosine deaminases responsible for RNA-editing reactions that occur within duplex RNA. Currently little is known regarding the nature of the protein-RNA interactions that lead to site-selective adenosine deamination. We previously reported that ADAR2 induced changes in 2-aminopurine fluorescence of a modified substrate, consistent with a base-flipping mechanism. Additional data have been obtained using full-length ADAR2 and a protein comprising only the RNA binding domain (RBD) of ADAR2. The increase in 2-aminopurine fluorescence is specific to the editing site and dependent on the presence of the catalytic domain. Hydroxyl radical footprinting demonstrates that the RBD protects a region of the RNA duplex around the editing site, suggesting a significant role for the RBD in identifying potential ADAR2 editing sites. Nucleotides near the editing site on the non-edited strand become hypersensitive to hydrolytic cleavage upon binding of ADAR2 RBD. Therefore, the RBD may assist base flipping by increasing the conformational flexibility of nucleotides in the duplex adjacent to its binding site. In addition, an increase in tryptophan fluorescence is observed when ADAR2 binds duplex RNA, suggesting a conformational change in the catalytic domain of the enzyme. Furthermore, acrylamide quenching experiments indicate that RNA binding creates heterogeneity in the solvent accessibility of ADAR2 tryptophan residues, with one out of five tryptophans more solvent-accessible in the ADAR2-RNA complex.

RNA editing is a term used to describe the structural alteration, insertion, or deletion of nucleotides in RNA that changes its coding properties (1). If the modification occurs in messenger RNA (mRNA), it can result in the translation of a protein sequence different from that predicted by the DNA sequence of the gene. Thus, this process plays an important role in creating functional diversity in the protein products of gene expression. Processing of the mRNA for mammalian GluR-B, a subunit of a glutamate-gated ion channel, involves editing reactions where genomically encoded sequences are altered in the pre-mRNA by adenosine deamination (2). The deamination of adenosine (A) in the mRNA results in inosine (I) at that position. Because inosine is translated as guanosine (G), the editing reaction causes a functional A to G replacement. For example, the R/G-editing site of the GluR-B pre-mRNA is located in an arginine codon that is converted to a sequence that encodes for

glycine. Receptors assembled with edited GluR-B subunits have been shown to recover from desensitization faster than receptors with arginine at this position (3). Specific deamination sites in other RNA sequences have also been identified (4, 5).

ADAR2 (adenosine deaminase that acts on RNA) is an ~80-kDa protein that efficiently deaminates the R/G site of GluR-B pre-mRNA sequences *in vitro* (6, 7). This enzyme has an RNA binding domain (RBD)¹ that includes two copies of the double-stranded RNA binding motif (dsRBM). The dsRBM is found in a number of double-stranded RNA-binding proteins such as PKR (the RNA-dependent protein kinase) and stauferin (a *Drosophila* RNA trafficking protein) (8). Consistent with the presence of dsRBMs in ADAR2, duplex RNA secondary structure in the substrate is a requirement for the ADAR2-catalyzed reaction. In the case of the R/G-editing site of the GluR-B pre-mRNA, this duplex is formed by the base-pairing of nucleotides at the 3' end of exon 13 and editing site complementary sequence found in intron 13 (3). C-terminal to the dsRBMs in ADAR2, amino acid sequences have been identified that may comprise the deamination active site (9, 10). Nucleoside deaminases such as adenosine deaminase (ADA) and cytidine deaminase have been extensively characterized structurally and mechanistically (11). The reactivity of substrate analogs implies that the deamination steps in the reaction mechanism for ADARs are similar to those found for the nucleoside deaminases (12). One major difference between the nucleoside deaminases and the ADARs is the requirement for duplex RNA structure in the ADAR substrate (13). The necessary trajectory of an attacking water molecule for hydrolytic deamination of adenosine makes it likely that the reactive nucleotide is flipped out of the duplex during reaction. Indeed, the fluorescence changes that occur when ADAR2 binds a 2-aminopurine-modified substrate are consistent with a base-flipping mechanism for this enzyme (14).

In this work, we describe experiments using R/G-editing site analogs derived from the GluR-B pre-mRNA in complex with full-length ADAR2 or the isolated RBD. These experiments demonstrate that the RBD has a specificity and affinity for duplex RNA similar to that of the full-length enzyme but cannot induce the structural change that leads to an increase in 2-aminopurine (2-AP) fluorescence. Furthermore, we observe a protein-dependent sensitivity to hydrolytic cleavage at nucleotides on the strand opposite the targeted adenosine, indicative of an increase in conformational flexibility of the RNA upon binding of the RBD. This is the first study to suggest that the RBD of an ADAR alters the conformational dynamics of the

* This work was supported by National Institutes of Health Grant GM-61115 (to P. A. B.). The costs of publication of this article were defrayed in part by the payment of page charges. This article must therefore be hereby marked "advertisement" in accordance with 18 U.S.C. Section 1734 solely to indicate this fact.

‡ To whom correspondence should be addressed. Tel.: 801-585-9719; Fax: 801-581-8433; E-mail: beal@chemistry.utah.edu.

¹ The abbreviations used are: RBD, RNA binding domain; ADAR, adenosine deaminase that acts on RNA; dsRBM, double-stranded RNA binding motif; PKR, RNA-dependent protein kinase; 2-AP, 2-aminopurine; GST, glutathione *S*-transferase; DTT, dithiothreitol; DS, double-stranded; SS, single-stranded.

RNA, indicating that this part of the protein plays more than just a recognition role in the ADAR2-editing reaction. Finally, analysis of the ADAR2 tryptophan fluorescence in the presence and absence of RNA indicates the protein undergoes conformational changes upon substrate binding. Acrylamide quenching suggests one of the five tryptophans in the catalytic domain is more exposed in the protein-RNA complex. These studies begin to shed light on the complex conformational changes that occur in both the protein and RNA during the RNA-editing adenosine deaminase reaction.

EXPERIMENTAL PROCEDURES

General—Distilled, deionized water was used for all aqueous reactions and dilutions. Biochemical reagents were obtained from Sigma/Aldrich unless otherwise noted. Common enzymes were purchased from Roche Molecular Biochemicals or New England Biolabs. Oligonucleotides were prepared on a PerkinElmer Life Sciences/ABI model 392 DNA/RNA synthesizer with β -cyanoethylphosphoramidites. Protected adenosine, guanosine, cytidine, uridine, and 2-aminopurine ribonucleoside phosphoramidites were purchased from Glen Research. [γ - 32 P]ATP (6000 Ci/mmol) and [5'- 32 P]pCp (cytidine 3',5'-bisphosphate) (3000 Ci/mmol) were obtained from PerkinElmer Life Sciences. Storage phosphor autoradiography was carried out using imaging plates obtained from Eastman Kodak Co. A Molecular Dynamics STORM 840 was used to obtain all data from phosphorimaging plates. Liquid scintillation counting was carried out with a Beckman LS 6500 scintillation counter and Bio-Safe II mixture from Research Products International Corp. PKR RBD was overexpressed in bacteria using pGEX-(His)₆-RBD and has been described previously (15). Full-length ADAR2 was overexpressed in *Saccharomyces cerevisiae* using the plasmid pScE[hA2a-His6] containing the human ADAR2 gene under the transcriptional control of a galactose-inducible GAL1 promoter. This expression system and the purification protocol employed were developed by Herbert L. Ley III and Prof. Brenda Bass, Dept. of Biochemistry, University of Utah (16).

Expression of the RBD of ADAR2—The human ADAR2 RBD (amino acids 71–316) was obtained as a glutathione *S*-transferase (GST) fusion protein by expression in *Escherichia coli* using derivatives of the bacterial expression plasmid pGEX-2T (Amersham Pharmacia Biotech). This fragment contains both dsRBMs and the intervening sequence (17). The following primers were used to amplify the RBD-coding sequence using the plasmid pScE[hA2a-His6] as template (16): 5' primer, 5'-GCGTGAaggatccAGGAAAACACCAGGGCCCCGTC-3'; 3' primer, 5'-TCACGCggtaccTTACTGAAGACCCTCACTGGGAAT-3'. Lowercase letters represent incorporated restriction sites (ADAR2 RBD template 5' primer *Bam*HI and 3' primer *Kpn*I). BL-21 *E. coli* (Amersham Pharmacia Biotech) cells were transformed with the ADAR2 RBD expression plasmid. A 5-ml overnight culture was used to inoculate 500 ml of media containing 16 g of bactotryptone, 10 g of yeast extract, 2.5 g of sodium chloride, 1 mM zinc sulfate, and 60 μ g of ampicillin at 37 °C. The culture was grown to an A_{600} between 0.5 and 0.6, at which point isopropylthiogalactopyranoside was added to a final concentration of 20 μ M. The induced culture was grown for an additional 20 h. The cells were collected by centrifugation and resuspended in 25 ml of phosphate-buffered saline, 1 mM phenylmethylsulfonyl fluoride, 1 mM DTT, and 100 μ g/ml lysozyme. The cell suspension was frozen at -80 °C followed by thawing at room temperature for 1 h. Cells were then lysed two times at 12,000 p.s.i. using a French pressure cell (Carver). The cell lysate was centrifuged at 16,000 \times *g* for 30 min at 4 °C. The clarified lysate was incubated with 1 ml of glutathione-Sepharose (Amersham Pharmacia Biotech) for 3 h at 4 °C. Unbound proteins were removed by 2 \times 20 ml and 5 \times 1 ml washes containing 20 mM Tris-HCl, pH 8.3, 300 mM NaCl, 1 mM DTT, 1 mM phenylmethylsulfonyl fluoride. The affinity matrix with bound GST-RBD was equilibrated with thrombin cleavage buffer (120 mM Tris-HCl, pH 8.6, 150 mM NaCl, 7 mM CaCl₂). The GST domain of the fusion protein was removed by cleaving with 0.5 units of thrombin (Amersham Pharmacia Biotech); the cleavage reaction was allowed to proceed for 18 h at 4 °C. Thrombin cleavage results in a protein with the sequence NH₂-GS(human ADAR2 (71–316))-COOH. To remove thrombin from the ADAR2 RBD, the supernatant was incubated with 600 μ l of benzamidine-Sepharose 6B (Amersham Pharmacia Biotech) pre-washed with 50 mM Tris-HCl, pH 8.0, containing 0.5 M NaCl. The supernatant was removed after 1 h of incubation at 4 °C. The matrix was washed with the above buffer, and the supernatants were combined. The purified protein was loaded into a 10,000-Da molecular mass cut-off Slide-A-Lyzer cassette (Pierce) and dialyzed overnight into 25 mM Tris-HCl, pH 7.0, 10 mM NaCl. The purity

of the ADAR2 RBD was estimated to be >95% based on analysis by Coomassie Blue-stained protein gels. A standard curve for protein concentration was generated by resolving known amounts of bovine serum albumin on a 10% SDS-polyacrylamide electrophoresis gel, visualizing the band by SyproOrange (Bio-Rad) staining, and quantifying the band intensities with a Molecular Dynamics STORM 840 PhosphorImager and ImageQuant software. All protein samples were separated into aliquots in 20–30- μ l fractions and stored at -20 °C.

Preparation of Duplex RNAs—Deprotection of synthetic oligoribonucleotides was carried out in 10 M CH₃NH₂ for 6 h at 35 °C followed by 0.1 M tetrabutylammonium fluoride in tetrahydrofuran for 8 h at 35 °C and desalted on Nap-10 columns (Amersham Pharmacia Biotech). Deprotected oligonucleotides were purified by polyacrylamide gel electrophoresis, visualized by UV shadowing, and extracted from the gel by the crush and soak method with 0.5 M NH₄OAc, 0.1% SDS, 0.1 mM EDTA. Extinction coefficients for absorbance at 260 nm for the RNAs were calculated as the sum of the extinction coefficients of the component nucleotides using 1000 cm⁻¹·M⁻¹ for 2-AP. A known amount of an oligonucleotide containing the 2-AP modification and a 1.5-fold excess of the complementary strand in 15 mM Tris-HCl, pH 7.5, 3% glycerol, 60 mM KCl, 1.5 mM EDTA, 0.003% Nonidet P-40, 0.3 mM DTT was heated at 85 °C and allowed to slow cool for 2.5 h until it reached room temperature for fluorescence experiments. For the formation of labeled duplex RNA, a given oligonucleotide was labeled at the 5' end using [γ - 32 P]ATP (6000 Ci/mmol) and T4 polynucleotide kinase or at the 3' end using [5'- 32 P]pCp (3000 Ci/mmol) and T4 RNA ligase (Amersham Pharmacia Biotech). Unincorporated [γ - 32 P]ATP or [5'- 32 P]pCp was removed using a Microspin G-25 column (Amersham Pharmacia Biotech). The labeled strand was first purified on a 15% denaturing polyacrylamide gel, excised, and extracted before it was hybridized to the unlabeled complement in TE buffer (10 mM Tris-HCl, pH 7.5, 0.1 mM EDTA) with 50 mM NaCl. The mixture was heated at 95 °C for 5 min and allowed to slow cool to room temperature. The duplex was purified on a 16% nondenaturing polyacrylamide gel. The appropriate band was visualized by storage phosphor autoradiography, excised, and extracted into TE buffer overnight at room temperature. Polyacrylamide particles were removed using a Spin-X (Costar) centrifuge column. The RNA duplex was ethanol-precipitated, redissolved in deionized water, and stored at -20 °C. The concentration was determined using scintillation counting and the specific activity of the labeled strand.

EDTA-Fe Footprinting—Varying amounts of protein, 25 nM duplex RNA, and 1 μ g/ml yeast tRNA^{Phe} in 6.7 mM Tris-HCl, pH 7.9, 27 mM KCl, 0.001% Nonidet P-40 were incubated for 5 min at 37 °C before final concentrations of 1.5 mM EDTA-Fe, 20 mM sodium ascorbate, and 0.3% H₂O₂ were added (20- μ l final reaction volume). The cleavage reactions were allowed to proceed for 10 min at 37 °C. The reaction was quenched with 5 μ l of a solution containing 50% glycerol and 1 mM EDTA. The RNA was extracted with phenol and chloroform and precipitated with 2 volumes of ethanol. The precipitated RNA was washed with 70 and 90% ethanol then denatured at 95 °C in 95% formamide and separated by electrophoresis on 16% denaturing polyacrylamide gel (29:1). Storage phosphorimaging plates were pressed flat against the polyacrylamide gels and exposed overnight. The cleavage data were analyzed and quantified using ImageQuant software.

RBD-induced Hydrolytic Cleavage—Varying amounts of protein, 25 nM duplex RNA, and 1 μ g/ml yeast tRNA^{Phe} were incubated for 5 min at 37 °C in 6.7 mM Tris-HCl, pH 7.5 or pH 9, 27 mM KCl, 0.001% Nonidet P-40. The final volume for each reaction was brought to 20 μ l, and incubation proceeded for an additional 10 min at 37 °C. The reaction products were treated as described above for EDTA-Fe cleavage experiments.

Fluorescence Measurements—Fluorescence measurements were performed utilizing an Instruments S. A., Inc., Fluorolog-3 spectrophotometer. Excitation was at 310 nm, and the fluorescence emission was scanned from 335 to 430 nm for 2-AP-containing RNAs. Spectra were obtained for solutions containing 0.8 μ M RNA, with increasing amounts of ADAR2 in 36 mM Tris-HCl, pH 7.5, 7% glycerol, 142 mM KCl, 3.6 mM EDTA, 0.01% Nonidet P-40, 0.7 mM DTT at room temperature. The fluorescence spectrum of the reaction buffer and enzyme was obtained and subtracted as background from all reactions. Slit widths of 5.0 nm were used for excitation and emission in all experiments. For the detection of tryptophan fluorescence, the excitation was at 295 nm, and the fluorescence emission was scanned from 330 to 355 nm. Spectra were obtained for solutions containing 400 nM ADAR2, with increasing concentrations of RNA. Tryptophan fluorescence quenching experiments with acrylamide were carried out by monitoring the change in the intensity at the emission maximum with increasing amounts of

acrylamide. Fluorescence quenching data were analyzed according to the Stern-Volmer equation (Equation 1) (18),

$$F_0/F = 1 + K_{sv}[Q] \quad (\text{Eq. 1})$$

where K_{sv} is the collisional Stern-Volmer constant, and F_0 and F are the fluorescence intensities of ADAR2 in the absence and presence of duplex RNA, respectively. $[Q]$ is the acrylamide concentration. A plot of F_0/F versus $[Q]$ yields a linear plot for homogeneous fluorescence emitters. A downward curvature of the Stern-Volmer plot indicates a heterogeneous population, *i.e.* only a fraction of the tryptophans is accessible to the quencher (19). The fraction of the initial fluorescence accessible to the quencher can be determined by using a modified Stern-Volmer equation (Equation 2),

$$F_0/(F_0 - F) = 1/([Q]f_a K_Q) + 1/f_a \quad (\text{Eq. 2})$$

where f_a is the fraction of the fluorophores accessible to quencher, and K_Q is the quenching constant. The plot of $F_0/(F_0 - F)$ versus $1/[Q]$ is linear, and the y intercept = $1/f_a$, whereas the slope = $1/f_a K_Q$.

Gel Mobility Shift Assays—To determine the dissociation constant (K_d) for ADAR2 RBD binding to the GluR-B duplex, varying amounts of RBD were added to 50 pM 5'-³²P end-labeled duplex in 15 mM Tris-HCl, pH 7.5, 3% glycerol, 60 mM KCl, 1.5 mM EDTA, 0.003% Nonidet P-40, and 0.5 mM DTT and incubated for 5 min at room temperature. To simulate conditions employed in the fluorescence experiments, binding reactions were carried out by combining 0.8 μM 5'-³²P end-labeled RNA duplex with varying concentrations of protein in 36 mM Tris-HCl, pH 7.5, 7% glycerol, 142 mM KCl, 3.6 mM EDTA, 0.01% Nonidet P-40, 0.7 mM DTT and allowing the mixture to incubate at room temperature for 5 min. Samples were then loaded onto a 6% nondenaturing polyacrylamide gel (79:1 acrylamide:bisacrylamide) and electrophoresed in 0.5× Tris-borate EDTA at 4 °C. Samples were loaded onto the gel while constant voltage was applied. Storage phosphorimaging plates were pressed flat against the polyacrylamide gels for exposure. The data were analyzed by performing volume integrations of the regions corresponding to free RNA, the ADAR2-RNA or RBD·RNA complex using the ImageQuant software. For the determination of dissociation constants, the data were fit to Equation 3 using the least-squares method of KaleidaGraph.

$$\text{Fraction bound} = [\text{RBD}]/([\text{RBD}] + K_d) \quad (\text{Eq. 3})$$

RESULTS

ADAR2 RBD Has an Affinity and Selectivity for Binding the R/G Duplex Similar to Full-length ADAR2—We demonstrated previously that when ADAR2 bound a duplex with 2-AP located at a position corresponding to the R/G-editing site of GluR-B pre-mRNA, the fluorescence emission maximum shifted 14 nm, and the intensity increased ~3.5-fold (14). This is consistent with ADAR2 flipping out the reactive nucleotide into a binding pocket similar in nature to that of the adenine N6 DNA methyltransferases (20, 21). To further define the structural features of the protein responsible for this effect, we carried out similar experiments using the isolated RBD of ADAR2 lacking the catalytic domain. ADAR2 RBD is defined here as the protein sequence that includes both dsRBMs and the intervening linker sequence (Fig. 1). For these experiments, we expressed a protein corresponding in sequence to human ADAR2 amino acids 71–316 as a GST fusion in *E. coli*. For analysis of the properties of the RBD, the GST domain was removed by specific proteolysis with thrombin. Gel mobility shift assays were performed to determine the dissociation constant (K_d) for binding to a substrate model of the GluR-B R/G site (*DS R/G*) (Fig. 1). The binding affinity of the RBD for this RNA ($K_d = 12 \pm 2$ nM) was found to be similar to that previously determined for full-length ADAR2 ($K_d = 22 \pm 4$ nM) (Fig. 2, A and B) (14).

To determine if ADAR2 RBD bound the RNA with any selectivity, we used EDTA·Fe to generate a hydroxyl radical footprint for this protein bound to the R/G site duplex. Previously, full-length rat ADAR2 was shown to protect a region of 16 nucleotides surrounding the R/G site using ribonuclease V1 footprinting (22). We observe a region of protection ~13 nucle-

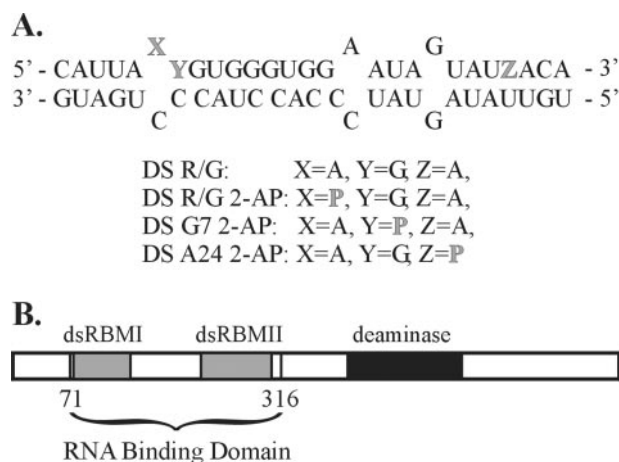


FIG. 1. A, duplex RNA ligands of ADAR2 used in this study. These duplexes are analogs of the R/G editing site of GluR-B pre-mRNA (3). *P* refers to 2-aminopurine ribonucleoside. B, domain structure of human ADAR2. dsRBMs are shown in gray, and the deaminase domain is indicated by black. Residues 71–316 constitute the RBD used in this study.

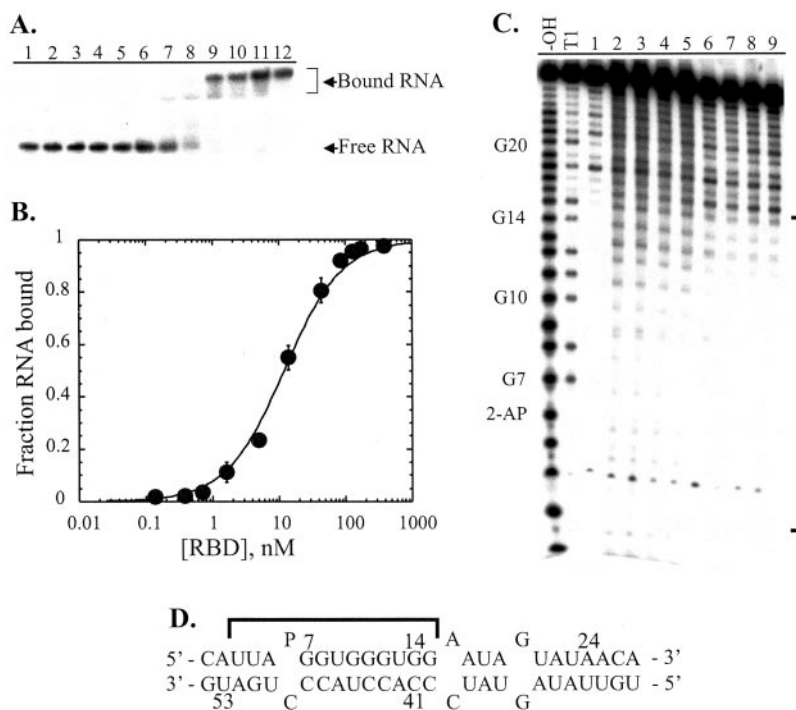
otides in length (U3-G15) on the edited strand near the editing site (Fig. 2, C and D). We also observe protection of over ~10 nucleotides on the non-edited strand (data not shown). Therefore, the RBD displays selective binding around the editing site on this duplex. The binding site observed here for ADAR2 RBD is similar to that detected for full-length rat ADAR2 and has been confirmed using affinity cleavage experiments with EDTA·Fe-modified RBD (22).² Interestingly, while carrying out footprinting experiments with ADAR2 RBD using a duplex with the non-edited strand labeled, we observed a protein-dependent hyperreactivity of nucleotides near the editing site (see below).

ADAR2 RBD Induces a Local Sensitivity to Hydrolytic Degradation of Duplex RNA—In addition to protection from cleavage by hydroxyl radical on the non-edited strand, we observed that some nucleotides on this strand near the editing site became hyperreactive in the presence of ADAR2 RBD (Fig. 3). This cleavage reaction is hydrolytic as it was not dependent on the presence of EDTA·Fe, was accelerated at higher pH, and the products comigrated with the products of RNase T1 and alkaline hydrolysis (for both 5' and 3' end-labeled RNA). This protein-induced hypersensitivity to hydrolytic cleavage is site-selective, as the cleavage sites were only present on the non-edited strand in a region near the edited adenosine and not found at any other site on the duplex (Fig. 3, B and C). Furthermore, this effect is specific to ADAR2 RBD, as the RNA binding domain from a different member of the dsRBM protein family, the RNA-dependent protein kinase, expressed and purified via similar methods as the ADAR2 RBD, did not induce the hyperreactivity (Fig. 3C).

Full-length ADAR2, but Not RBD, Site-selectively Enhances the Fluorescence of a 2-Aminopurine-containing RNA Duplex—2-AP is a fluorescent adenosine analog whose quantum yields and emission λ_{max} are sensitive to its electronic environment (23). Single-stranded oligonucleotides containing 2-AP are highly fluorescent; however, when present in a base-paired duplex, the 2-AP fluorescence is quenched. Together, these properties have made 2-AP a useful probe for the base-flipping step in the reactions of nucleic acid-modifying enzymes (20, 24–26). When full-length human ADAR2 is added to duplex RNA with 2-AP at the R/G-editing site, the measured fluorescence intensity increases (14). Fluorescence intensities ob-

² O. M. Stephens and P. A. Beal, manuscript in preparation.

FIG. 2. *A*, quantitative gel mobility shift analysis of the binding of RBD to the DS R/G duplex. Shown is the storage phosphor autoradiogram of the gel used to separate bound from free RNA; lanes 1–12: 0, 0.1, 0.4, 0.7, 1.6, 5.0, 14, 43, 86, 129, 172, and 387 nM RBD added. *B*, plot of the fraction RNA bound as a function of RBD concentration. The data were fit to the equation, fraction bound = $[RBD]/([RBD] + K_d)$, using the least squares method of KaleidaGraph. Data points reported are the average \pm S.D. for three independent experiments. *C*, hydroxyl radical cleavage of the 5' end-labeled 2-AP-containing strand of 25 nM DS R/G 2-AP was investigated in the presence of increasing amounts of RBD. The protected nucleotides are identified with a bracket. Lane 1, RNA with no added hydrogen peroxide or EDTA-Fe; lanes 2–9 correspond to the addition of 0, 4, 9, 15, 25, 42, 70, and 116 nM RBD; -OH, alkaline hydrolysis; T1, T1 RNase. *D*, mapping of the protection of the duplex in the presence of RBD.



served when various concentrations of ADAR2 were added to a solution of 0.8 μ M DS R/G 2-AP are shown in Fig. 4A. Also plotted is the fractional saturation of the RNA by the protein under the same conditions measured by a gel shift assay. As can be seen from this analysis, the observed increase in fluorescence intensity correlates with RNA binding, with the maximum intensity occurring when the RNA is maximally bound. When 1.8 μ M ADAR2 was added to 0.8 μ M DS R/G 2-AP, the emission intensity increased 4.2-fold, and the emission maximum shifted to 359 nm as reported previously (Fig. 4, A and B) (14). To determine if these fluorescence changes were localized to the editing site, the concentration of ADAR2 that gave the maximum fluorescence change with the DS R/G 2-AP substrate was used with substrates DS G-7 2-AP and DS A-24 2-AP, where the 2-AP is located at nucleotide positions not modified by the enzyme (Fig. 1A). When ADAR2 was added to these other modified substrates, little change in the 2-AP fluorescence was detected (Fig. 4B). The change observed with these substrates was similar to that observed with single-stranded RNA with 2-AP at the R/G-editing site (SS R/G 2-AP). Importantly, when ADAR2 RBD was added to these various RNAs, little change in fluorescence was observed. To ensure that this was not due to differences in binding, gel mobility shift assays were performed under the conditions of the fluorescence measurements (Fig. 4C). We found that the fractional saturation of 2-AP modified RNA by various concentrations of RBD was similar to that observed for full-length ADAR2 (Fig. 4C). Therefore, even though ADAR2 RBD is capable of high affinity and selective binding to the RNA duplex, it cannot induce the conformational change that leads to an increase in 2-AP fluorescence.

Duplex RNA Induces Changes in the Tryptophan Fluorescence of ADAR2—The binding of ADAR2 to double-stranded RNA was also examined by measuring changes in tryptophan fluorescence. All five of the tryptophans present in the human ADAR2 sequence are located within the C-terminal catalytic domain (17). Therefore, any change in tryptophan fluorescence observed upon substrate binding would likely arise from conformational changes occurring in the catalytic domain. In the presence of a saturating amount of dsRNA (200

nM), we observed a 20% enhancement in emission without detectable change in either peak shape or maximum ($\lambda_{em} = 345$ nm) (Fig. 5A). Single-stranded RNA was used as a control for the tryptophan fluorescence experiments, and no enhancement in emission was observed, as might be expected for a double-stranded RNA binding protein. The fraction of RNA bound by ADAR2 under gel shift conditions shows that up to 200 nM RNA gives maximal binding to the amount of ADAR2 present in the tryptophan fluorescence assay (400 nM), and addition of more duplex RNA leads to the appearance of free RNA in the gel (Fig. 5B). The concentration of RNA that gives the maximum binding by gel shift also gives the maximum enhancement in tryptophan fluorescence. Interestingly, when additional RNA is added beyond this point, we see a decrease in fluorescence to a level that is \sim 10% higher than the value with no RNA added, and no further changes with additional RNA added beyond that point (Fig. 5A).

Acrylamide Quenching of Tryptophan Fluorescence Indicates Heterogeneity of Accessibility of Tryptophans in the ADAR2-RNA Complex—Acrylamide quenching was employed to assess the solvent accessibility of the five tryptophans present in the ADAR2 catalytic domain (27). Acrylamide was chosen as a quencher for tryptophan residues because it is uncharged; thus, it should be able to collide with tryptophan whether it is on the surface or in the interior of a protein. A Stern-Volmer plot shows that tryptophan quenching by acrylamide is homogeneous for ADAR2 alone (Fig. 6A). However, the tryptophan fluorescence of the ADAR2-RNA complex is more highly quenched at low acrylamide concentrations followed by relative insensitivity at higher acrylamide concentrations, leading to an overall downward curvature of the Stern-Volmer plot (Fig. 6A). Thus, the data for the ADAR2-RNA complex were re-plotted using a modified Stern-Volmer plot because the downward curvature suggested the tryptophans were not equally accessible to the quencher (18). The reciprocal of the y intercept represents the fraction of the initial fluorescence accessible to the quencher (19). A y intercept of 4.4 ± 0.1 was obtained, the reciprocal of which gives an accessible fraction of $22.8 \pm 0.1\%$ (Fig. 6B). Thus, if all the tryptophans

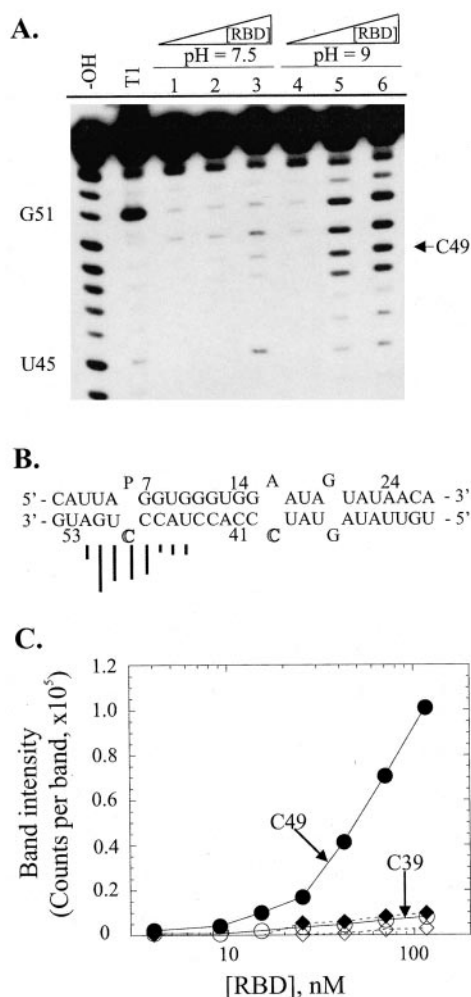


FIG. 3. *A*, hydrolytic cleavage of the non-edited strand of 25 nM DS R/G 2-AP; lanes 1–3 correspond to the addition of 0, 42, and 70 nM RBD at pH 7.5; lanes 4–6 correspond to the addition of 0, 42, and 70 nM RBD at pH 9; -OH, alkaline hydrolysis; T1, RNase T1. *B*, mapping of the nucleotides that become sensitive to hydrolytic cleavage in the presence of RBD. The length of the bar represents the cleavage band intensity at that position. **Bold** indicates nucleotides C-39 and C-49, whose band intensities were quantified as a function of RBD concentration in *C*. *C*, the observed sensitivity to hydrolytic cleavage is selective for nucleotides near the editing site and specific to ADAR2 RBD. A plot of the intensity of the cleavage band (PhosphorImager counts) corresponding to C-49 (●) and C-39 (◆) in the presence of various concentrations of ADAR2 RBD (solid line) and at C-49 (○) and C-39 (◇) in the presence of various concentrations of PKR RBD (broken line).

contribute equally to the observed fluorescence, one out of five is more solvent-accessible in the ADAR2-RNA complex.

DISCUSSION

Sequence analysis of the C termini of known adenosine deaminases that act on RNA revealed the presence of motifs similar to those found in the family of adenine N6 DNA methyltransferases (10). These conserved motifs include amino acids that were shown in the crystal structure of the methyltransferase M·TaqI in complex with duplex DNA to make up the binding site for the flipped out deoxyadenosine (21, 25). In addition, adenine N6 DNA methyltransferases have been shown to induce an increase in 2-AP fluorescence, with a blue shifted emission λ_{\max} for 2-AP-modified substrates (20, 25). We have shown previously that ADAR2 induces similar changes in the fluorescence properties of RNA substrates, with 2-AP located at an editing site (14). In the absence of a high resolution structure of the complex between ADAR2 and a duplex RNA substrate, we cannot rule out that the increase in 2-AP fluo-

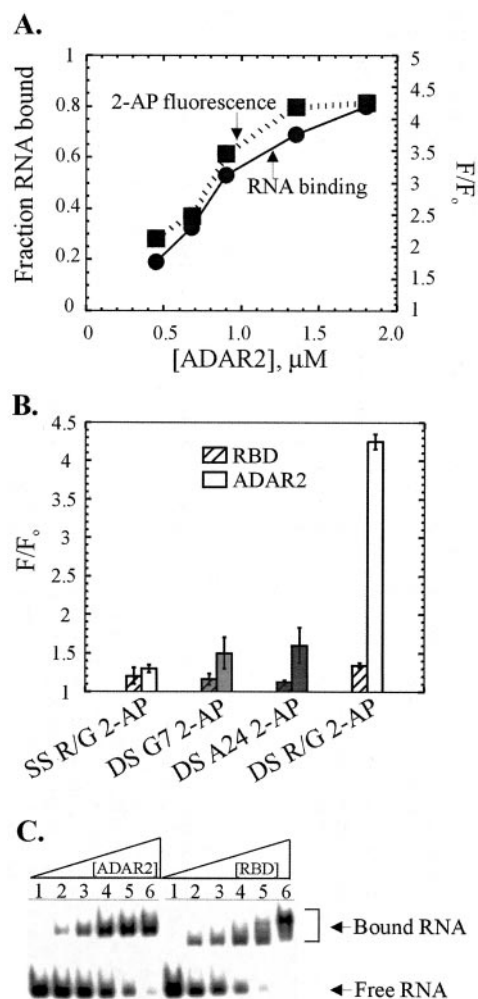


FIG. 4. *A*, plot of the fraction of 0.8 μM DS R/G 2-AP bound as a function of increasing amounts of ADAR2 (solid line) and a plot of the increase in fluorescence of DS R/G 2-AP as a function of titrated ADAR2 (broken line). *B*, bar graph depicting the positional dependence for 2-AP fluorescence increase as well as the role of the RBD with 0.8 μM RNA and 1.8 μM ADAR2 or RBD. *C*, gel mobility shift analysis of the binding of ADAR2 and RBD to DS R/G 2-AP substrate under the conditions of the 2-AP fluorescence measurements; lanes 1–6 correspond to the addition of 0, 0.5, 0.7, 0.9, 1.4, and 1.8 μM protein.

rescence arises from severe bending or other distortion in the RNA structure that leads to an unstacking of the 2-AP. However, given the similarities in 2-AP fluorescence changes observed with ADAR2 and with adenine N6 DNA methyltransferases, enzymes that have been shown to base flip by high resolution structural analysis (21), we interpret these fluorescence changes as arising from ADAR2-induced base flipping, where the 2-AP is extruded from the duplex and placed in a hydrophobic active site pocket. In this paper, we sought to further characterize the conformational changes occurring when ADAR2 binds duplex RNA. RNAs with the 2-AP at different locations as well as a fragment of ADAR2 consisting of only the RBD were studied by gel shift assays, footprinting, and by monitoring 2-AP fluorescence changes. In addition, tryptophan fluorescence changes were measured upon RNA binding to assess any protein conformational changes that may take place.

Interestingly, although gel mobility shift assays and EDTA-Fe footprinting studies indicated that the RBD of ADAR2 alone bound a model RNA substrate with high affinity and selectivity, this protein was unable to cause the 2-AP fluorescence changes (Figs. 2 and 4). Therefore, protein struc-

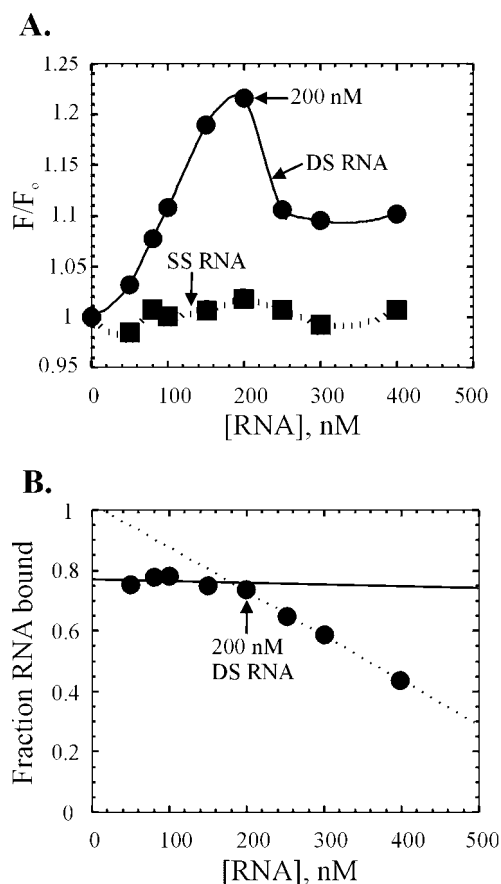


FIG. 5. A, plot of the change in tryptophan fluorescence of 400 nM ADAR2 with increasing amounts of double-stranded RNA (DS R/G) (●) and single-stranded RNA (SS R/G) (■). B, fraction of DS R/G duplex bound to 400 nM ADAR2 with increasing concentrations of added RNA under the conditions of tryptophan fluorescence measurements obtained using a gel mobility shift assay.

ture required for the conformational change that leads to the increase in 2-AP fluorescence lies outside the RBD. Given that the RBD does not contain the sequence motifs conserved in the adenine N6 DNA methyltransferases, a likely explanation of this result is that the RBD does not contain the binding site for the flipped out adenosine. However, the RBD did induce hydrolytic cleavage of nucleotides on the strand opposite the edited base, suggesting an alteration in the RNA structure at that site (Fig. 3). Since protein-induced hyperreactive nucleotides were observed, further investigation was necessary to determine if this could be due to ribonuclease contamination. Several facts, however, argue against ribonuclease contamination as the source of this cleavage reaction. First, the cleavage was highly localized, with reactive nucleotides present on the non-edited strand opposite the editing site, with no other cleavage sites observed on this duplex. Second, the efficiency of the reaction showed an RBD concentration dependence similar to that of RNA binding as measured by EDTA-Fe footprinting and gel shift assays. Third, the RNA binding domain of a different member of the dsRBM protein family, the RNA dependent protein kinase, expressed and purified via similar methods as the ADAR2 RBD, does not induce the hyperreactivity observed (Fig. 3C). The cleavage reaction was determined to be hydrolytic in nature as the products comigrated with RNase T1 and alkaline hydrolysis products for both 5' and 3' end-labeled RNAs. Also, it was found that the cleavage efficiency could be controlled by an increase or decrease in pH of the reaction, with higher yields at higher pH. All these results lead to the conclusion that the cleavage observed is due to an RBD-induced

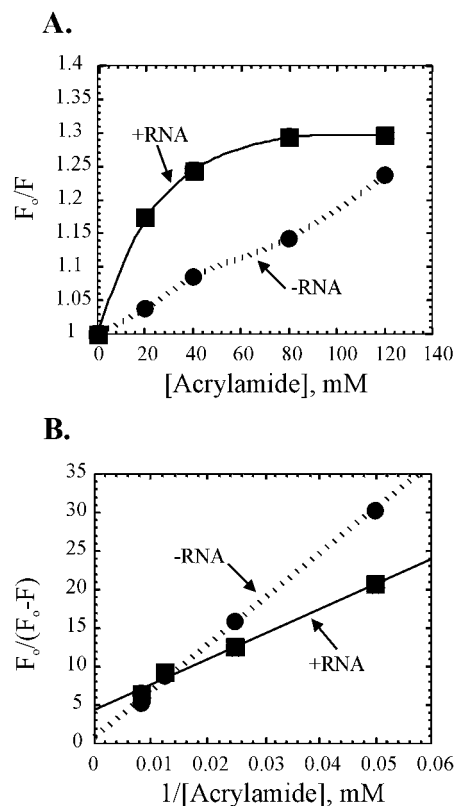


FIG. 6. Acrylamide quenching study of tryptophan fluorescence using 400 nM ADAR2 and 200 nM DS R/G. A, Stern-Volmer plot of acrylamide quenching in the presence (■) and (●) absence of RNA. The downward curvature is indicative of a heterogeneous population of tryptophans. B, modified Stern-Volmer plot in the presence (■) and (●) absence of RNA.

increase in the sensitivity to hydrolytic degradation of the RNA localized on the non-edited strand near the editing site. Regions of structured RNAs that are sensitive to hydrolytic cleavage have been shown to have a high degree of flexibility. For instance, hydrolytic degradation has been observed in crystals of tRNAs in the flexible loops (28). Given that this reaction occurred in the crystal, nuclease contamination could be ruled out. The degradation patterns observed correlate with the observed crystallographic temperature factors, consistent with conformational flexibility as a key factor controlling the degradation reaction. This flexibility allows for the proper alignment of the attacking 2'-hydroxyl to be in line with the phosphodiester bond to be broken during the cleavage reaction (28, 29). Our interpretation of an RBD-induced increase in hydrolytic cleavage of the RNA is that RBD increases the conformational flexibility of the nucleotides around the editing site. This would have the effect of lowering the energy barrier to base flipping during the ADAR reaction. Studies with uracil DNA glycosylase suggest that the duplex structure of the DNA is destabilized before base flipping (24). For many of the known and proposed base-flipping enzymes, the interstrand separation of the phosphodiester backbones is proposed to lower the activation energy barrier required for base flipping (30, 31). Interestingly, when full-length ADAR2 binds, no hyperreactivity is observed. This may be due to the large catalytic domain enclosing the duplex, so as to mask the effect of the RBD alone. Therefore, the sensitivity to hydrolytic cleavage of the RNA upon protein binding observed here with RBD would never be observed naturally when full-length ADAR2 binds pre-mRNA substrates.

How does ADAR2 preferentially and specifically deaminate

certain adenosines? There are two contrasting theories as to how DNA modifying enzymes find their specific substrate; they are processive and non-processive extrusion (32). In the processive extrusion mechanism, the enzyme migrates along the DNA helix and sequentially flips out each base until a target base is encountered (32). Under the non-processive mechanism, the enzyme randomly samples bases until the target base is inserted into the active site. ADARs, much like DNA modifying enzymes, could locate their substrate by a processive extrusion mechanism where each base is sampled by the active site of the enzyme. However, our fluorescence data do not support processive extrusion by ADAR2, since the replacement of guanosine 7 and adenosine 24 with 2-AP shows minimal protein-induced increases in fluorescence intensity or shifts in emission maxima (Fig. 4B). Thus, the distinct footprint seen with RBD around the editing site and the fluorescence increase only at the targeted nucleotide appear to support a mechanism in which RBD directs the catalytic domain to a specific location on the duplex to flip a nucleotide into the active site. Recently, Lazinski and co-workers (33) demonstrated that a protein chimera containing the ADAR2 catalytic domain and the ADAR1 RBD maintained the substrate selectivity observed for ADAR2 (and not that of ADAR1), indicating that the catalytic domain of ADAR2 contributes significantly to the selectivity of the enzyme (33). Thus, ADAR2 selectivity for certain adenosines within duplex RNA substrates appears to involve a combination of selective binding on the RNA by the RBD as well as complementarity between the RNA structure surrounding the adenosine and the catalytic domain.

Tryptophan fluorescence emission spectra of proteins are sensitive to changes in the tryptophan environment and can be a valuable tool for studying protein conformation changes upon ligand binding in solution using relatively little enzyme (27). When a solution of ADAR2 was titrated with a duplex RNA ligand, the tryptophan fluorescence steadily increased until it reached a maximum ~20% higher than that of the protein alone (Fig. 5A). The amount of RNA necessary to achieve the maximum fluorescence intensity correlated with the amount of RNA necessary to saturate the protein (Fig. 5B). Human ADAR2 contains five tryptophan residues, all of which are present in the catalytic domain of the protein. Thus, any change in the tryptophan fluorescence can be attributed to changes in the catalytic domain upon substrate binding. One explanation for the observed increase is the movement of a tryptophan away from protonated amino acids, such as arginine or lysine, which can quench tryptophan fluorescence (19, 34). Importantly, when the M·EcoRI adenine N6 DNA methyltransferase bound DNA, a 45% increase in tryptophan fluorescence was observed (34). This enzyme has two tryptophans in its sequence, and the increase has been shown to arise from changes in the environment of Trp-183. Crystal structures of a related adenine N6 DNA methyltransferase (M·TaqI) free and bound to DNA clearly show that the protein undergoes conformational changes in two loops upon DNA binding, one of which takes part in the formation of the binding pocket for the flipped out deoxyadenosine (21). Our acrylamide-quenching data suggest that one of the five tryptophan residues in the catalytic domain of ADAR2 becomes more exposed upon binding RNA (Fig. 6). RNA binding to ADAR2 may cause a conformational change similar to that observed with M·TaqI, preferentially exposing one of its five tryptophans.

The maximum tryptophan fluorescence of 400 nm ADAR2 was observed with the addition of 200 nm RNA (Fig. 5). Therefore, the complex formed could have a ratio of ADAR2:RNA equal to 2:1. However, this interpretation would require that the ADAR2 sample used for these experiments be 100% active.

At this time, we cannot rule out a 1:1 ADAR2:RNA stoichiometry, which would indicate that the ADAR2 sample used contained 50% active sites. Also, we do not understand fully why additional RNA leads to a decrease in fluorescence to a level 10% higher than that of the protein alone. It may be that the addition of excess RNA leads to a non-productive binding mode, and this binding mode has a quenching effect on the fluorescence of the productive ADAR2-RNA complex.

In summary, our results have identified the RBD of ADAR2 as playing two roles, a role in recognition of potential ADAR2 editing sites and an additional role in rendering the nucleotides around the targeted adenosine more conformationally flexible, thus lowering the activation energy for base flipping. However, protein structure outside of the RBD is required to cause the conformational change that leads to the 2-AP fluorescence increase indicative of base flipping. In addition, data obtained with 2-AP-substituted substrates suggest the enzyme does not employ a processive extrusion mechanism. Last, the effect RNA has on ADAR2 tryptophan fluorescence suggests the protein undergoes a conformational change when it binds duplex RNA, likely involving the exposure of one of the five tryptophans in the catalytic domain.

Acknowledgments—We thank Prof. Brenda Bass and Herbert L. Ley III in the Department of Biochemistry, University of Utah for the expression plasmid pScE[hA2a-His₆].

REFERENCES

- Grosjean, H., and Benne, R. (1998) *Modification and Editing of RNA*, pp. 551–553, American Society for Microbiology, Washington, D. C.
- Higuchi, M., Single, F. N., Kohler, M., Sommer, B., Sprengel, R., and Seeburg, P. H. (1993) *Cell* **75**, 1361–1370
- Lomeli, H., Mosbacher, J., Melcher, T., Hoger, T., Geiger, J. R., Kuner, T., Monyer, H., Higuchi, M., Bach, A., and Seeburg, P. H. (1994) *Science* **266**, 1709–1713
- Polson, A. G., Bass, B. L., and Casey, J. L. (1996) *Nature* **380**, 454–456
- Burns, C. M., Chu, H., Rueter, S. M., Hutchinson, L. K., Canton, H., Sander-Bush, E., and Emeson, R. B. (1997) *Nature* **387**, 303–308
- O'Connell, M. A., Gerber, A., and Keller, W. (1997) *J. Biol. Chem.* **272**, 473–478
- Melcher, T., Maas, S., Herb, A., Sprengel, R., Seeburg, P. H., and Higuchi, M. (1996) *Nature* **379**, 460–464
- Fierro-Monti, I., and Mathews, M. B. (2000) *Trends Biochem. Sci.* **25**, 241–246
- Lai, F., Drakas, R., and Nishikura, K. (1995) *J. Biol. Chem.* **270**, 17098–17105
- Hough, R. F., and Bass, B. L. (1997) *RNA (N. Y.)* **3**, 356–370
- Carter, C. W., Jr. (1995) *Biochimie (Paris)* **77**, 92–98
- Easterwood, L. M., Veliz, E. A., and Beal, P. A. (2000) *J. Am. Chem. Soc.* **122**, 11537–11538
- Polson, A. G., Crain, P. F., Pomerantz, S. C., McCloskey, J. A., and Bass, B. L. (1991) *Biochemistry* **30**, 11507–11514
- Stephens, O. M., Yi-Brunozzi, H. Y., and Beal, P. A. (2000) *Biochemistry* **39**, 12243–12251
- Vuyisich, M., and Beal, P. A. (2000) *Nucleic Acids Res.* **28**, 2369–2374
- Ley, H. L., III (2001) *Editing of Hepatitis Delta Virus Antigenomic RNA by Recombinant Human Adenosine Deaminases That Act on RNA*. Ph.D. thesis, University of Utah
- Yang, C.-C., Sklar, P., Axel, R., and Maniatis, A. (1997) *Proc. Natl. Acad. Sci. U. S. A.* **94**, 4354–4359
- Lehrer, S. S. (1971) *Biochemistry* **10**, 3254–3263
- Lakowicz, J. R. (1999) in *Principles of Fluorescence Spectroscopy*, 2nd Ed., Klumer Academics/Plenum Press, New York
- Allan, B. W., and Reich, N. O. (1996) *Biochemistry* **35**, 14757–14762
- Goedecke, K., Pignot, M., Goody, R. S., Scheidig, A. J., and Weinhold, E. (2001) *Nat. Struct. Biol.* **8**, 121–125
- Ohman, M., Kallman, A. M., and Bass B. L. (2000) *RNA (N. Y.)* **6**, 687–697
- Ward, D. C., Reich, E., and Stryer, L. (1969) *J. Biol. Chem.* **244**, 1228–1237
- Stivers, J. T., Pankiewicz, K. W., and Watanabe, K. A. (1999) *Biochemistry* **38**, 952–963
- Holz, B., Klimasauskas, S., Serva, S., and Weinhold, E. (1998) *Nucleic Acids Res.* **26**, 1076–1083
- Allan, B. W., Reich, N. O., and Beechem, J. M. (1999) *Biochemistry* **38**, 5308–5314
- Eftink, M. R., and Ghiron, C. A. (1976) *Biochemistry* **15**, 672–680
- Dock-Bregeon, A. C., and Moras, D. (1987) *Cold Spring Harbor Symp. Quant. Biol.* **52**, 113–121
- Vlassov, V. V., Zuber, G., Felden, B., Behr, J.-P., and Giege, R. (1995) *Nucleic Acids Res.* **23**, 3161–3167
- Klimasauskas, S., and Roberts, R. J. (1995) *Nucleic Acids Res.* **23**, 1388–1395
- Cal, S., and Connolly, B. A. (1997) *J. Biol. Chem.* **272**, 490–496
- Verdine, G. L., and Bruner, S. D. (1997) *Chem. Biol. (Lond.)* **4**, 329–334
- Wong, S. K., Sato, S., and Lazinski, D. W. (2001) *RNA (N. Y.)* **7**, 846–858
- Maeigley, K. A., Gonzalez, L., Jr., Smith, D. W., and Reich, N. O. (1992) *J. Biol. Chem.* **267**, 18527–18532